Full Text View

Volume 30, Issue 6 (June 2000)

Journal of Physical Oceanography
Article: pp. 1281–1304 | Abstract | PDF (374K)

A Two-Dimensional Time-Dependent Model of a Wind-Driven Coastal Polynya: Application to the St. Lawrence Island Polynya

M. A. Morales Maqueda* **and A. J. Willmott**

Department of Mathematics, Keele University, Keele, Staffordshire, United Kingdom

(Manuscript received November 9, 1998, in final form July 18, 1999)

DOI: 10.1175/1520-0485(2000)030<1281:ATDTDM>2.0.CO;2

ABSTRACT

A two-dimensional time-dependent model of a wind-driven coastal polynya is presented. The model combines and extends previous one-dimensional time-dependent and two-dimensional steady-state flux formulations. Given the coastline geometry, and the time-varying surface winds and heat fluxes as free parameters, the model calculates the growth rate, distribution and motion of frazil ice within the polynya, and the mass fluxes of frazil ice and consolidated new ice at the polynya edge. The difference between these two mass fluxes determines the velocity of the polynya edge at all times and, hence, its evolution. Analytical solutions are found for the special case when the coastline is a straight line segment of finite length D (an idealization of an island) and the forcing fields are spatially uniform and constant in time. Two timescales and two spatial scales are shown to be important in characterizing the shape, size, and evolution of the polynya: the consolidated new ice and frazil ice timescales, t_{ce} and t_{fe}, respectively, and the offshore and alongshore adjustment length scales, R_{oe} and R_{ae}, respectively. The timescale t_{ce} is the time required for the polynya to grow ice of thickness equal to the collection thickness of frazil at the polynya edge. The timescale t_{fe} is the time it takes frazil to cross the equilibrium width of the polynya, which is, in turn, determined by the length scale R_{oe}. In combination, t_{ce} and t_{fe} control the timescale for the polynya to respond to variations in the forcing. The length scale R_{ae} is the distance that the angle between the consolidated new ice and frazil ice drifts spans along the equilibrium polynya edge. This length scale measures the sensitivity of the polynya edge to alongshore variations in the coastline geometry and, in particular, to its total extent. It is shown that if R_{ae} is comparable to D, then the offshore dimension of the polynya and the timescale for the polynya to reach equilibrium can be very different from those obtained from a one-dimensional formulation. The model is applied to the study of seasonal and short-term variability of the St. Lawrence Island polynya, in the Bering Sea.

1. Introduction

A feature of the sea ice cover over shallow coastal areas is the appearance of wind-driven polynyas, regions of partially ice-free waters that form between the coastline and the ice pack as a result of the wind-driven offshore advection of ice. As

the the pack is pushed away from the coast, an area of open water is left behind in which frazil ice formation occurs. Because the coastal shelf is not very deep, the entire water column is usually near the freezing point and no oceanic heat flux is supplied from below. Frazil ice growth rates over the polynya region can therefore be very large (up to several meters of ice per year; Schumacher et al. 1983). The frazil ice created is also transported downwind and it eventually collects along the trailing ice floes at the polynya edge. The size and shape of the polynya are governed by the balance between the export of new ice out of the polynya and the production of frazil ice within the polynya. Wind-driven polynyas tend to form recurrently in specific locations of the Arctic Ocean, the sub-Arctic seas, and the Southern Ocean. Depending on the coastline geometry and the environmental conditions, their widths range from hundred or thousands of meters to a hundred kilometers (Smith et al. 1990).

Wind-driven polynya models developed to date fall into two categories, namely, grid models and flux balance models. Grid models employ finite difference formulations of sea ice thermodynamics and dynamics in order to determine the ice growth and motion in the area of the polynya (e.g., Lynch et al. 1997; Fichefet and Goosse 1999). On the other hand, flux balance models are based on the idea of Lebedev (1968) that the balance between the flux of frazil ice produced in the polynya and the wind-driven offshore divergence of ice governs the location of the polynya edge. These kind of models are the subject of our present study.

We distinguish two regions in a wind-driven coastal polynya (Fig. 1a): (i) an inner region of nearly open water where frazil ice grows and (ii) an outer region surrounded by first-year ice pack and occupied by a mat of consolidated new ice and young ice floes that have formed by accretion of frazil ice arriving from region (i). We will refer to region (i) as the "polynya," proper, and the boundary between regions (i) and (ii) will be termed the "polynya edge." The goal of a flux model is to predict the location and temporal evolution of the polynya edge.

Based on the flux balance principle, Pease (1987) introduced a one-dimensional time-dependent model of a wind-driven polynya. In this model, all the frazil ice produced within the polynya is assumed to be instantaneously collected at the polynya edge. In other words, the net frazil ice production in the polynya is exactly balanced by the net flux of ice out of the polynya, namely

$$FR = H\left(U - \frac{dR}{dt}\right), \qquad (1)$$

where F is the frazil ice production rate (volume of ice grown per unit area per unit time), R is the polynya width, and H and U are the collection thickness of frazil ice and the consolidated new ice velocity at the polynya edge, respectively. In (1), it is assumed that the frazil ice growth rate within the polynya is spatially uniform. Ou (1988) extended the previous model to include a finite drift rate for frazil ice. In this case, an equation for dR/dt is derived by exploiting the balance between the fluxes of frazil ice and consolidated new ice at the polynya edge:

$$h_R\left(u_R - \frac{dR}{dt}\right) = H\left(U - \frac{dR}{dt}\right), \qquad (2)$$

where h_R and u_R are the frazil ice depth and the frazil ice velocity at the polynya edge, respectively. If the frazil ice velocity field is specified, h_R can be obtained from the continuity equation for frazil ice depth, h, subject to the boundary condition $h = 0$ at the coast.

The theory of Pease (1987) provides expressions for the steady-state width and the equilibrium timescale of a polynya under constant forcing. The steady-state polynya width is $R_{oe} = HU/F$. The equilibrium timescale is a small multiple (3 or 4, say) of $t_{ce} = H/F$, which is simply the e-folding time implied by (1). This timescale is of the order of several hours to one day. Pease tested the model for winter conditions in the Bering Sea and reached two major conclusions: (i) the polynya width is only moderately sensitive to wind speed since both ice drift and frazil ice production vary linearly with the wind stress magnitude and (ii) the polynya width is very responsive to surface air temperatures. The latter is due to the fact that air temperatures strongly affect the frazil ice production but not the ice drift (e.g., colder air leads to larger ice growth and a smaller polynya for a given wind). Ou (1988) showed in turn that, when a finite frazil ice drift is taken into account, (i) the time required for the polynya to reach equilibrium is shorter than in the formulation of Pease (1987) and that (ii) normally a polynya is in approximate equilibrium with synoptic (of the order of days) atmospheric variations and its width is therefore reasonably described by the steady-state polynya width.

The one-dimensional model of Pease (1987) has been applied in a number of studies. Mysak and Huang (1992) used the model to simulate the formation and maintenance of the North Water polynya. They coupled the Pease (1987) model to a reduced-gravity ocean model, and showed that, in addition to the short-period timescale t_{ce}, a second long-period timescale (of the order of weeks) exists, associated with the influence of oceanic heat flux on the frazil ice production rate. Markus and Burns (1995) discussed satellite-derived estimates of the location and extent of a polynya near Halley Bay, Antarctica, and compared them with the theory of Pease (1987). The model exhibited reasonable skill in reproducing the area fluctuations of the polynya. Kozo et al. (1990) used a purely advective polynya model in which the polynya size is the product of the consolidated ice velocity and the duration of an offshore wind episode. Their analysis suggested that polynya size is reasonably well correlated to observed geostrophic winds over the Bering Sea.

A two-dimensional steady-state polynya flux model was discussed by Darby et al. (1994). They assumed that the frazil ice moves at a fixed angle to the right of the surface wind and with a speed proportional to the wind speed. This polynya model was coupled to a reduced-gravity ocean model and used to determine the area of the North Water polynya. The coupled model did not take into account the influence of ocean currents on frazil ice motion. The general theory for a two-dimensional steady-state polynya flux model was expounded by Darby et al. (1995). The steady-state polynya edge is described by the curve $C(\mathbf{R}) = \text{const}$, where $\mathbf{R}$ is the position of a point of the polynya edge. The polynya edge is determined by requiring the normal fluxes of frazil and consolidated new ice across the polynya edge to be in balance:

$$\mathbf{n}_C \cdot (H\mathbf{U} - h_C\mathbf{u}_C) = 0, \quad (3)$$

where $\mathbf{n}_C$ is a unit vector perpendicular to the polynya edge, and H, $\mathbf{U}$, h_C, and $\mathbf{u}_C$ are the collection thickness of frazil ice, the consolidated new ice velocity, the frazil ice thickness, and the frazil ice velocity at the polynya edge, respectively. As in the one-dimensional case, if the frazil ice velocity field is known over the entire domain, h_C can be determined by solving the continuity equation for frazil ice depth, h, inside the polynya, with $h = 0$ at the coast.

In addition to the offshore equilibrium length scale, R_{oe}, the two-dimensional theory introduces an alongshore adjustment length scale, R_{ae}, which is proportional to R_{oe} but which also depends on the directions of drift of frazil and consolidated new ice relative to each other and to the coastline. Darby et al. (1995) showed that the polynya edge shape is insensitive to coastline features with length scales smaller than R_{ae}. In Darby et al. the frazil ice motion was prescribed to be rectilinear. Willmott et al. (1997) allowed frazil ice to move along curvilinear trajectories that were determined via the free-drift momentum balance approximation.

In this paper, we formulate a two-dimensional time-dependent polynya flux model. The model requires the specification of the coastline boundary and of time-varying surface wind, shortwave radiation, air temperature, and relative humidity. The model calculates ice production and drift rates, which allow the temporal evolution of the polynya edge to be determined. The model is applied to the investigation of the seasonal and short-term variability of the St. Lawrence Island polynya.

The paper is organized as follows. Section 2 provides a formulation of the polynya model and outlines the numerical method for determining the solution. Section 3 presents analytical and numerical polynya solutions in the presence of idealized coastlines. Section 4 discusses the application of the model to the simulation of the St. Lawrence Island polynya. Section 5 closes the paper with a summary and some concluding remarks.

2. Description of the model

Figure 1b shows a schematic diagram of the polynya model. For a wind blowing offshore, frazil ice is formed in the polynya region (i) and is transported toward the consolidated new ice region (ii), where it collects alongside the ice floes. The polynya edge is represented by the curve $C(\mathbf{R}, t) = \text{const}$, where $\mathbf{R}$ is the position vector of a point of the polynya edge. (A list of the most relevant variables used in the paper can be found in the appendix.) The evolution of the polynya edge can be determined if the thickness, h, and velocity, $\mathbf{u}$, of frazil ice, the frazil ice collection thickness at the polynya edge, H, and the velocity of the consolidated new ice, $\mathbf{U}$, are known. In general, all the above quantities are functions of both space and time. Note that h and H are not in situ ice thicknesses; that is, they do not denote the actual ice thickness at a given point, rather they represent the volume of ice per unit area in a vicinity of that point. For instance, inside the polynya, a significant amount of frazil ice is kept in suspension within the water column (Omstedt and Svensson 1984) and the surface ice is very often collected in Langmuir wind rows. Within this context, the concept of an in situ frazil ice thickness is not suitable. Likewise, the downwind consolidated new ice region is normally perforated with numerous holes and, therefore, H is more appropriately viewed as an area-averaged thickness (Pease 1987).

Using a generalization of (2), the evolution equation for the polynya edge is

$$\nabla C \cdot \frac{H\mathbf{U} - h_C\mathbf{u}_C}{H - h_C} + \frac{\partial C}{\partial t} = 0, \quad (4)$$

where ∇ is the two-dimensional gradient operator and h_C and $\mathbf{u}_C$ are the frazil ice thickness and velocity at the polynya edge, respectively. Equation (4) can be solved using the method of characteristics (e.g., Haberman 1998). The characteristic curves of (4) satisfy

$$\frac{d\mathbf{R}}{dt} = \frac{H\mathbf{U} - h_C\mathbf{u}_C}{H - h_C}. \quad (5)$$

Since the polynya edge is not a material surface, only the component of $d\mathbf{R}/dt$ perpendicular to the polynya edge is physically relevant. Denoting by $\mathbf{n}_C$ a unit vector perpendicular to $C(\mathbf{R}, t)$ and pointing toward the consolidated new ice region, we see that, when the polynya reaches equilibrium, $\mathbf{n}_C \cdot d\mathbf{R}/dt = 0$, which is equivalent to (3). Note also that whether ice convergence or ice divergence occurs at the polynya edge depends on whether $\mathbf{n}_C \cdot (\mathbf{u}_C - \mathbf{U})$ is greater or smaller than zero, respectively. In the latter case, $h_C = 0$ and, from (5), $d\mathbf{R}/dt = \mathbf{U}$.

The evolution of h, $\mathbf{u}$, H, and $\mathbf{U}$ is determined as follows. The distribution of frazil ice within the polynya can be obtained from the following system of equations:

$$\frac{d\mathbf{r}}{dt} = \mathbf{u}, \qquad \frac{dh}{dt} = F - h\nabla \cdot \mathbf{u}. \qquad (6)$$

In (6), $\mathbf{r}$ is the position vector along a frazil ice trajectory and F is the frazil ice production rate. If the spatial and temporal distributions of $\mathbf{u}$ are known, the characteristics of the frazil ice depth equation coincide with the frazil ice trajectories. Frazil ice trajectories can in principle emanate not only from the coast, but also from regions of the polynya edge where ice divergence occurs, and this is shown schematically in Fig. 1b. In all cases, for $t > t_0$, where t_0 is the initial time, the boundary condition for h at points where a frazil ice trajectory emanates is $h = 0$.

Since the extent of synoptic atmospheric systems is much larger than typical polynya length scales, we assume that the atmospheric forcing is uniform over the polynya and, consequently, that freezing rates are also uniform. Following Pease (1987), the frazil ice production is determined as

$$-\rho_i L_i F = (1-\alpha)Q_s + \sigma e_a T_a^4 - \sigma e_s T_w^4 + \rho_a C_h C_p U_a (T_a - T_w) + \rho_a C_e L_e U_a (q_a - q_s), \qquad (7)$$

where α is the water surface albedo, Q_s is the downwelling shortwave radiation, σ (=5.67 × 10^{-8} W m^{-2} K^{-4}) is the Stefan–Boltzmann constant, e_a is the air emissivity, T_a is the air temperature, e_s (=0.97) is the surface emissivity, T_w (=−1.8°C) is the water temperature, ρ_a (=1.3 kg m^{-3}) is the air density, C_h (=1.75 × 10^{-3}) is the sensible heat transfer coefficient, C_p (=1004 J K^{-1} kg^{-1}) is the specific heat for air, U_a is the wind speed, C_e (=1.75 × 10^{-3}) is the latent heat transfer coefficient, L_e is the latent heat of vaporization (=2.5 × 10^6 J kg^{-1}), q_a is the mixing ratio at T_a, q_s is the saturated mixing ratio at T_w, ρ_i (=950 kg m^{-3}) is the ice density, and L_i (=3.34 × 10^5 J kg^{-1}) is the ice latent heat of fusion. The above parameter values have been taken from Fichefet and Morales Maqueda (1997), except that for ρ_i, which comes from Pease (1987). Both the short and longwave radiations absorbed at the surface strongly depend on cloud coverage, type and optical thickness, and α, Q_s, and e_a are therefore functions of these cloud variables. However, Pease neglects altogether the shortwave radiation contribution, on the basis that it is very small from October throughout February, and ignores cloud effects on downwelling longwave radiation by adopting a constant atmospheric emissivity e_a = 0.95. This author also neglects surface latent heat fluxes.

The frazil ice drift field can exhibit complex spatial patterns, even when a spatially uniform wind forcing is imposed. For winds of 3 m s^{-1} or faster, frazil ice has been observed to drift along wind rows associated with Langmuir circulations (Martin and Kauffman 1981). These wind rows are oriented at an angle, θ, of 13° or less to the right of the wind (in the Northern Hemisphere) and their spacing oscillates between 2 and 200 m (Leibovich 1983). Since the persistence time of the wind rows (of the order of 1 h) is normally shorter than the residence time of frazil ice within a mature polynya, it is reasonable to assume that the existence of Langmuir circulation structures does not lead to any net horizontal convergence or divergence of frazil ice within the polynya. According to Leibovich (1983), typical windward Langmuir currents have speeds that are a few percent of the wind speed. Correspondingly, we prescribe

$$\mathbf{u} = \epsilon_L [\cos(\theta)\mathbf{U}_a - \sin(\theta)\mathbf{k} \times \mathbf{U}_a], \qquad (8)$$

where ϵ_L (=0.06) is a constant of proportionality, θ (=0°) is a turning angle positive to the right of the wind (in the Northern Hemisphere), $\mathbf{k}$ is an upward unit vector, and $\mathbf{U}_a$ is the surface wind velocity.

The physical processes governing the collection of frazil ice at the polynya edge are not well understood, although the frazil ice collection thickness is expected to depend on wind speed and fetch (Bauer and Martin 1983; see section 5). Following Pease (1987), we use a constant value for H (=0.1 m), which, if thermodynamic growth of consolidated new ice is neglected, represents the area-averaged thickness of ice in region (ii).

Finally, the drift of consolidated new ice is parameterized by Zubov's law (Wadhams 1986):

$$\mathbf{U} = \epsilon_Z [\cos(\Upsilon)\mathbf{U}_a - \sin(\Upsilon)\mathbf{k} \times \mathbf{U}_a], \qquad (9)$$

where ϵ_Z (=0.03) is a constant of proportionality and Υ (=28°) is a turning angle positive to the right of the wind (in the Northern Hemisphere). Note that, since, in the Arctic, the observed surface geostrophic wind velocity makes an angle of 23°–33° to the right of a $\mathbf{U}_a$ (Overland and Colony 1994), the consolidated ice drift will be approximately aligned with the geostrophic wind (which is another way of stating Zubov's law).

In order to solve (5) and (6), it is necessary to specify the location of the polynya edge, $C(\mathbf{R}, t)$ = const for $t \leqslant t_0$. In addition, knowledge of $H(\mathbf{R}, t)$, $\mathbf{U}(\mathbf{R}, t)$, $\mathbf{u}(\mathbf{r}, t)$, and $F(\mathbf{r}, t)$ is required for all t, both $t \leqslant t_0$ and $t > t_0$. This is because we

do not make any particular assumption regarding the initial state of the polynya. Since the thickness of frazil ice at the polynya edge depends on the history of the ice as it drifts offshore, we need, in general, to be able to compute the frazil ice trajectories for all times. Of course, this will not be necessary in the special, but very important, case when the polynya was closed for $t \leqslant t_0$. For arbitrary coastline geometry and forcing fields, the polynya equations have to be solved numerically. This is done in the following manner. Suppose that the solution algorithm has determined the location of the polynya edge at times t_0, $t_1 = t_0 + \Delta t$, $\cdots$, $t_{N-1} = t_0 + (N-1)\Delta t$, where Δt is the time step. To advance the solution from t_{N-1} to $t_N = t_0 + N\Delta t$, a series of M points, $\mathbf{R}^1_{N-1}$, $\cdots$, $\mathbf{R}^M_{N-1}$, along the polynya edge at time t_{N-1} is selected. Consider the point $\mathbf{R}^k_{N-1}$ ($1 \leqslant k \leqslant M$). If ice divergence occurs at $\mathbf{R}^k_{N-1}$ (i.e., frazil ice is leaving the polynya edge), then $h^k_{N-1} = 0$, and $[d\mathbf{R}/dt]^k_{N-1} = \mathbf{U}^k_{N-1}$, where h^k_{N-1} and $\mathbf{U}^k_{N-1}$ are, respectively, the frazil ice depth and the consolidated new ice velocity at $\mathbf{R}^k_{N-1}$ at time t_{N-1}. If ice convergence occurs at $\mathbf{R}^k_{N-1}$ (i.e., frazil ice is arriving at the polynya edge), then h^k_{N-1} has to be calculated in order to determine $[d\mathbf{R}/dt]^k_{N-1}$. To find h^k_{N-1}, the first of (6) is integrated backward in time until, at a time $t_{\text{int}} \leqslant t_{N-1}$, the frazil ice trajectory first intersects a boundary point, **P**, from which frazil ice emerges. Note that **P** can be located either on the coastline or on a sector of the polynya edge where ice divergence occurs. In the latter case, owing to the fact that, in general, t_{int} will not coincide with any of the times t_0, $\cdots$, t_{N-1}, the location of the polynya edge at t_{int}, and hence **P**, will have to be determined by interpolation of the known polynya edge solutions at the consecutive times t_j and t_{j+1}, where $t_j \leqslant t_{\text{int}} \leqslant t_{j+1}$. Since the trajectory followed by frazil ice from **P** at time t_{int} to $\mathbf{R}^k_{N-1}$ at time t_{N-1} is known (i.e., we assume that **u** does not depend on h), the second of (6) can be integrated forward in time, with initial condition $h(\mathbf{P}, t_{\text{int}}) = 0$, to obtain h^k_{N-1}. Thus, $[d\mathbf{R}/dt]^k_{N-1}$ can now be calculated from (5), and the polynya edge solution advanced from $\mathbf{R}^k_{N-1}$ to $\mathbf{R}^k_N$.

3. Polynya solutions for uniform forcing and idealized coastlines

To facilitate understanding of the time-dependent behavior of a two-dimensional wind-driven coastal polynya, we present a number of analytical and numerical polynya solutions for simple coastline geometries. In all cases, the atmospheric forcing fields (i.e., the air temperature and wind velocity), and hence F, **u**, and **U**, are assumed to be spatially uniform. We use a Cartesian coordinate frame, S, in which the coordinates of a point on the polynya edge will be denoted by (X, Y) and those of a point along a frazil ice trajectory by (x, y). With respect to S, the consolidated new ice velocity is (U, V) and the frazil ice velocity is (u, v). Equations (5) and (6) then become

$$\frac{dX}{dt} = \frac{HU - h_C u}{H - h_C}, \qquad \frac{dY}{dt} = \frac{HV - h_C v}{H - h_C}, \tag{10}$$

$$\frac{dx}{dt} = u, \qquad \frac{dy}{dt} = v, \qquad \frac{dh}{dt} = F. \tag{11}$$

a. Infinite straight coastline: Polynya response to an impulsive change in the forcing

Consider an infinite straight coastline, which coincides with the y axis, and with the polynya occupying the region $x \geqslant 0$. Given a point, **P**, with coordinates (x_P, y_P), the set of points (x_P, y) will be said to be located to the "west" ("east") of **P** if $y - y_P < 0$ ($y - y_P > 0$). Similarly, the points (x, y_P) will be said to be located to the "north" ("south") of **P** if $x - x_P < 0$ ($x - x_P > 0$). Assume that for $t < t_0$ a polynya exists in equilibrium with an atmospheric forcing, with $\mathbf{U} = \mathbf{U}_0$, $\mathbf{u} = \mathbf{u}_0$, and $F = F_0$. The polynya edge at $t = t_0$ is given by the infinite straight line $[X]_{t=t_0} = X_0 = (U_0 H)/F_0$. At $t = t_0$, the distribution of h within the polynya is given by $h(x, t_0) = [(h_{C0} - h_{B0})/X_0]\, x + h_{B0}$, where $h_{C0} = (F_0/u_0)\, X_0$ and $h_{B0} = 0$ are the initial thicknesses of frazil ice at the polynya edge and at the coast, respectively. In section 3c, an example arises in which $0 \leqslant h_{B0} \leqslant h_{C0}$ occurs during the evolution of a two-dimensional polynya, which is the reason for allowing $h(x, t_0)$ to depend on h_{B0}.

Assume that at $t = t_0$ the atmospheric forcing changes impulsively and that, for $t \geqslant t_0$, the consolidated new ice velocity, frazil ice velocity, and frazil ice production acquire new values **U**, **u** and F, respectively. In essence, this problem is one-dimensional in the x direction and has been solved by Ou (1988). Nevertheless, we will revisit this problem because the methodology used to solve it is the same as that employed in the case of a finite-length straight coastline. Unfortunately, the location of the polynya edge cannot, in general, be expressed as an explicit function of t. However, since H, **U**, **u**, and F are constant for $t \geqslant t_0$, the only time-dependent variable controlling the polynya edge evolution is h_C. We will therefore first solve (10) and (11) for h_C as an implicit function of t. In so doing, we will be able to define as well a timescale for the polynya to reach the new equilibrium state. Subsequently, h_C will be introduced back into (10) in order to determine the location of the polynya edge as an explicit function of h_C. The characteristic length scales of the steady-state polynya will

also be derived. Finally, we will discuss some salient features of the polynya solutions thus obtained.

1) EVOLUTION OF H_C AND DETERMINATION OF THE POLYNYA EQUILIBRIUM TIMESCALE

Take a point (X, Y) of the polynya edge at time $t \geq t_0$. The thickness of frazil ice arriving at the polynya edge point at time t is given by

$$h_C(X, Y, t) = \begin{cases} \dfrac{h_{C0} - h_{B0}}{X_0}[X - u(t - t_0)] + h_{B0} + F(t - t_0), & t < t_c, \quad (12a) \\ \dfrac{F}{u}X, & t \geq t_c, \quad (12b) \end{cases}$$

(Click the equation graphic to enlarge/reduce size)

where t_c is such that $[X - u(t - t_0)]_{t=t_c} = 0$. In words, t_c is the time after which all frazil ice particles arriving at the polynya edge have been exposed only to the new forcing (Ou 1988).

It is expedient to define the new variable $p = 1 - h_C/H$. Physically, the frazil ice cannot be thicker than its collection thickness and, therefore, $0 \leqslant p \leqslant 1$. This inequality imposes a restriction on the possible values of h_{B0}, which we will not consider here. This restriction is overcome by using a parameterization for H along the lines of the one outlined in section 5. By eliminating X between (10) and (12), an evolution equation for p is formed whose solution is given by

$$\begin{cases} \dfrac{F}{H}(t - t_0) = -(p - p_0) - Zp_e \ln\dfrac{Zp_e - p}{Zp_e - p_0}, & t < t_c, \quad (13a) \\ \dfrac{F}{H}(t - t_c) = -(p - p_c) - p_e \ln\dfrac{p_e - p}{p_e - p_c}, & t \geq t_c, \quad (13b) \end{cases}$$

where $p_0 = [p]_{t=t_0}$, $Z = u(h_{C0} - h_{B0})/(FX_0)$, $p_e = 1 - U/u$, and $p_c = [p]_{t=t_c}$.

The value of t_c can be obtained as follows. From (12a) we find that, when $t \longrightarrow t_c$, with $t < t_c$, then $p \longrightarrow p'_c = 1 - h_{B0}/H - F/H(t_c - t_0)$ (note that $p'_c = p_c$ if and only if $h_{B0} = 0$). By taking the limit $t \longrightarrow t_c$ in (13a), and setting $p = p'_c$ in the resulting equation, we obtain an expression for t_c, namely

$$\frac{F}{H}(t_c - t_0) = 1 - \frac{h_{B0}}{H} - Zp_e + (Zp_e - p_0)\exp\left(-\frac{FX_0/(uH)}{p_e}\right). \quad (14)$$

A timescale for the polynya to reach its new equilibrium can be found from (13b) by determining the time, $t = t_\epsilon \geq t_c$, at which the value of p is $p_\epsilon = [p]_{t=t_\epsilon}$, where $p_e - p_\epsilon = \epsilon(p_e - p_c)$, and $0 < \epsilon \ll 1$. We find that

$$\frac{F}{H}(t_\epsilon - t_0) = 1 - [1 - \ln(\epsilon^{-1})]p_e + \epsilon(p_e - p_c). \quad (15)$$

If the polynya was closed at $t = t_0$, then $p_c = 1$ and the definition of p_ϵ is equivalent to $R_{oe} - X_\epsilon = \epsilon R_{oe}$, where $R_{oe} = HU/F$ is the steady-state polynya width and $X_\epsilon = [X]_{t=t_\epsilon}$. In this case, t_ϵ is the time required for the polynya to open to a width $(1 - \epsilon)R_{oe}$.

In practice, if $h_{B0} = 0$, the equilibrium adjustment timescale in (15) can be approximated by $F/H(t_\epsilon - t_0) \approx 1 - [1 - \ln(\epsilon^{-1})]p_e$. We observe that this approximation is independent of the initial state of the polynya. It is also interesting to note that the approximation can be expressed in terms of the two timescales $t_{ce} = R_{oe}/U = H/F$ and $t_{fe} = R_{oe}/u$ in the following way:

$$t_\epsilon - t_0 \approx t_{fe} + \ln(\epsilon^{-1})(t_{ce} - t_{fe}). \quad (16)$$

The timescale t_{fe} is simply the time required for frazil ice to traverse the width of the equilibrium polynya, R_{oe}. The timescale $t_{ce} = H/F$ is the time required for the polynya to grow frazil ice up to a thickness H. If we choose $\epsilon = 0.01$, (16) leads to the following bounds for the adjustment timescale: $H/F \leqslant t_\epsilon - t_0 \leqslant 4.6H/F$. The lower bound is the finite adjustment timescale in the limit $p_e \to 0$, or equivalently $t_{fe} \to t_{ce}$ (in fact, the only case when the adjustment timescale is finite corresponds to this limit), while the upper bound corresponds to the limit $p_e \to 1$ (i.e., $U \to 0$ or $u \to \infty$).

2) EVOLUTION OF THE POLYNYA EDGE AND DETERMINATION OF THE POLYNYA CHARACTERISTIC LENGTH SCALES

We now derive expressions for X and Y in terms of p. Changing independent variable in (10) from t to p gives differential equations for X and Y, which are separable in p. The solutions are

$$\begin{cases} \dfrac{F}{uH}(X - X_0) = -\left[p - p_0 + (Zp_e - p_e)\ln\dfrac{Zp_e - p}{Zp_e - p_0}\right], & t < t_c, \\ \dfrac{F}{uH}(X - X_c) = -(p - p_c), & t \geq t_c, \end{cases} \quad (17)$$

$$\begin{cases} \dfrac{F}{vH}(Y - Y_0) = -\left[p - p_0 + (Zp_e - q_e)\ln\dfrac{Zp_e - p}{Zp_e - p_0}\right], & t < t_c, \\ \dfrac{F}{vH}(Y - Y_c) = -\left[p - p_c + (p_e - q_e)\ln\dfrac{p_e - p}{p_e - p_c}\right], & t \geq t_c, \end{cases} \quad (18)$$

where $Y_0 = [Y]_{t=t_0}$, $Y_c = [Y]_{t=t_c}$, and $q_e = 1 - V/v$. Equations (13), (14), and (17) uniquely determine the polynya width, X, as a function of t. An initial polynya edge point (X_0, Y_0) will transform into a point (X, Y) at time t according to (13), (14), (17), and (18). The path followed by such point during its evolution is termed a characteristic. Figure 2 depicts the polynya edge evolution to equilibrium for a case in which the polynya was initially closed ($p_0 = p_c = 1$). The ice speeds are $|\mathbf{U}| = 0.6$ m s^{-1} and $|\mathbf{u}| = 2|\mathbf{U}|$. The frazil ice production is $F = 0.27$ m day^{-1}.

Let us now consider the steady-state polynya solution in order to determine its characteristic length scales. From (10) and (11), the steady-state polynya width, R_{oe}, is given by

$$R_{oe} = HU/F. \quad (19)$$

In addition to R_{oe}, an alongshore adjustment length scale, R_{ae}, can also be defined. To understand how R_{ae} arises, suppose that in the interval $I = \{y : y_1 < y < y_2\}$ the infinite-length coastline exhibits small departures from the straight line boundary $x = 0$. Specifically, let the coastline be given by $x = c(y)$, where c is such that $c = 0$ outside I and $|c| \ll R_{oe}$. We assume that $|dc/dy| \ll 1$, in order to guarantee that frazil ice trajectories starting at a given point of the land boundary will not subsequently intercept the coastline again. The coordinates of any point $\mathbf{Q}$ on the steady-state polynya edge can be written as $(X = X_e + X', Y)$, where $X_e = R_{oe}$ and X' ($|X'| \ll R_{oe}$) is a perturbation induced by the coastline irregularities. It can be shown that a frazil ice trajectory arriving at the equilibrium point $\mathbf{Q}$ emanates from a coastal point $\mathbf{P}$ whose x coordinate is $x'_P \approx c(Y - v/uR_{oe})$, to first order in the perturbation. The thickness of frazil ice arriving at $\mathbf{Q}$ is then $h_C = h_{Ce} + h'_C$, where $h_{Ce} = HU/u = (F/u)\,R_{oe}$ and $h'_C = (F/u)(X' - x'_P)$, where $X' - x'_P$ is the "excess offshore distance" traveled by frazil ice due to the perturbation in the coastal outline. We next observe that, dividing the first of (10) by the second of (10), we obtain an expression for the slope of the steady-state polynya edge, dX/dY, as a function of h_C [to convince oneself that this is indeed the equation for the steady-state polynya edge, one has simply to set $\partial C/\partial t = 0$ in (4)]. An equation for the polynya edge perturbation readily follows and is given by

$$R_{oe}\left(\frac{\upsilon}{u} - \frac{V}{U}\right)$$

to first order in the perturbation. In (20), the denominator

$$R_{ae} = R_{oe}\left(\frac{\upsilon}{u} - \frac{V}{U}\right) \qquad (21)$$

is an alongshore adjustment length scale. There is a useful geometrical interpretation of the length scale R_{ae}, as illustrated in Fig. 2. Consider a consolidated new ice trajectory and a frazil ice trajectory both emanating from the same point on the coastline [e.g., the point $(0,\ y_1)$ in Fig. 2]. The length of the line segment defined by the two points where these two trajectories intercept $X = R_{oe}$ is given by $|R_{ae}|$.

Given that the angle between **U** and **u** is positive (i.e., **U** is located to the right of **u**), the steady-state polynya edge solution east of the semi-infinite straight line $l_2 = \{(x,\ y)\ :\ \upsilon x - u(y - y^2) = 0, x \geq 0\}$ will be the same as in the case of a perfectly straight coastline, namely, $X = R_{oe}$. Equation (20) can then be integrated westward from the point ($X_0 = R_{oe}$, $Y_0 = y_2 + \upsilon/uR_{oe}$), where $X' = 0$, thereby showing that

$$X' = -\exp\left(-\frac{Y_0 - Y}{R_{ae}}\right)\int_{Y_0}^{Y}\frac{c\left(Z - \frac{\upsilon}{u}R_{oe}\right)}{R_{ae}}\exp\left(\frac{Y_0 - Z}{R_{ae}}\right)dZ. \qquad (22)$$

It is clear from (22) that R_{ae} fulfills a twofold role. On the one hand, it controls the amplitude, $|X'|$, of the polynya edge response to a perturbation in the coastline shape [in the integrand of (22), the coastline perturbation $c(y)$ is scaled by a factor $1/R_{ae}$]. On the other hand, R_{ae} also provides an e-folding length scale for the westward decay of X' (due to the presence of the exponential outside the integral). In Fig. 2, for example, the perturbation will decay by e^{-1} over a distance $|R_{ae}|$ westward of the line l_1. Modifications in the coastline with offshore and alongshore length scales smaller than R_{ae} will barely affect the polynya edge shape.

3) DISCUSSION OF POLYNYA SOLUTIONS

The time-dependent polynya behavior crucially depends on the orientations of both the consolidated new ice and frazil ice velocities. This is illustrated in Figs. 3 and 4, which show results from two series of polynya experiments. In each experiment, for $t < t_0 = 0$ the polynya is in a steady state in which the ice drift is characterized by the velocities $\mathbf{U}_0$ ($|\mathbf{U}_0| = 0.6$) and $\mathbf{u}_0$ ($|\mathbf{u}_0| = 2|\mathbf{U}_0|$). The frazil ice production rate is $F = 0.27$ m day^{-1}. An impulsive change in wind direction occurs at $t = t_0$ and the consolidated new ice and frazil ice velocities become $\mathbf{U}_1$ and $\mathbf{u}_1$, respectively. The wind speed and air temperature remain constant and, therefore, $|\mathbf{U}_1| = |\mathbf{U}_0|$ and $|\mathbf{u}_1| = |\mathbf{u}_0|$. When the polynya attains its new equilibrium state [within 1% of $p_e - p_c$; see (15)], the forcing reverts to the "old" wind regime for $t < t_0$, the consolidated new ice and frazil ice velocities becoming $\mathbf{U}_2 = \mathbf{U}_0$ and $\mathbf{u}_2 = \mathbf{u}_0$, respectively.

Figure 3 shows the polynya width as a function of time when the angle between the consolidated new ice and frazil ice drifts, Φ, is 0°. The evolution of the polynya width in time is shown for five different orientations of $\mathbf{U}_0$ and $\mathbf{u}_0$, with $\mathbf{U}_1$ and $\mathbf{u}_1$ held constant. In all cases, the polynya edge takes ~ 24 h to advance to its new steady state after the first impulsive change in wind direction. The retreat phase after the second change in wind direction also lasts for ~ 24 h. This 24-h timescale agrees well with the one obtained from (15) or (16) with $\epsilon = 0.01$ and $p_e = 0.5$. Since the behavior of the polynya depends only on the magnitude of the offshore components of the consolidated new ice and frazil ice velocities, the evolution of the polynya edge is identical when $\mathbf{U}_0/\mathbf{u}_0$ make an angle $\pm\beta$ with the normal to the coastline, provided $|\mathbf{U}_0|$ and $|\mathbf{u}_0|$ are constant (cf. Figs. 3b and 3e, and Figs. 3c and 3d). However, this symmetry is broken if Φ is nonzero. For example, in Fig. 4, $\Phi = +28°$ and, when the polynya evolves to an equilibrium state in which $\mathbf{U}_1$ is normal to the coastline, $p_e = 1 - 1/\cos(28°) \approx 0.43$, and $t_\epsilon \sim$ 23 h. The time required for the polynya to return to its initial state varies according to the direction of $\mathbf{U}_0$ (=$\mathbf{U}_2$), from ~ 41 h when $\mathbf{U}_0$ is parallel to the coast ($p_e = 1$) to ~ 9 h when $\mathbf{U}_0$ forms an angle, β, with the normal to the coastline of +39° ($p_e = 0$). For $\beta > +39°$, $U > u$, and the steady-state polynya width is unbounded because no equilibrium of ice fluxes at the polynya edge is possible.

The transient behavior of the polynya can be such that the polynya opening (closing) is preceded by a partial closing (opening). This can be understood as follows. If the polynya is in equilibrium for $t < t_0$, the flux balance at the polynya edge is $M = HU_0 - h_{C0}u_0 = 0$, where $h_{C0} = [h_C]_{t=t_0}$. If the offshore components of the ice drift regime change impulsively to U and u, the flux balance at $t = t_0$ is $M = Hu(U/u - U_0/u_0)$. Whether the polynya width increases or decreases during the transient adjustment depends on whether the sign of $U/u - U_0/u_0 = p_0 - p_e$ is positive or negative, respectively.

b. Finite-length straight coastline: Polynya response to an impulsive change in the forcing

Consider the case when the coast is a finite-length straight-line segment coinciding with the y axis and with end points (0, 0) and (0, D). A coastline of this type can be viewed as an idealization of a long and narrow island. Let us assume that the polynya forms to the south of the island, occupying a finite-area region of the half-plane $0 \leqslant x$. We will first study the case when the polynya opens to equilibrium from an initial state in which the polynya was closed. A complete analytical solution will be obtained for this case. Subsequently, we will examine the response of a steady-state polynya of nonzero area to an impulsive change in the forcing. This more general problem introduces novel polynya features, which are worthwhile discussing. The polynya equations for this case can also be solved analytically. However, the complete construction of the analytical solution becomes intractable, and therefore a numerical procedure is adopted for solving this problem.

1) RESPONSE OF A POLYNYA INITIALLY CLOSED AND DETERMINATION OF THE POLYNYA EQUILIBRIUM TIMESCALES

Let us suppose that for $t < t_0$ the entire oceanic domain is covered by motionless first-year ice. At $t = t_0$, a steady wind is applied and a polynya opens to the south of the coastline. We assume that, when the first-year ice is free to move, its velocity is the same as that of the consolidated new ice exported from inside the polynya [see (9)] and that it is stationary when its advance is hindered by the coastline. That is, we assume an idealized ice rheology in which the ice resists convergence with arbitrarily large compressive strength and opposes no resistance to divergence or shearing. In this approach, a region of motionless first-year ice exists north of the island bounded by the coastline to the south and by the semi-infinite lines $L^- = \{(X, Y) : VX - UY = 0, X < 0\}$ to the west and $M^- = \{(X, Y) : VX - U(Y - D) = 0, X < 0\}$ to the east (Fig. 5). Elsewhere, the ice cover moves in free drift. The boundaries between the motionless and the moving first-year ice (i.e., L^- and M^-) can be considered as coastline extensions along which the polynya width is zero.

According to (10), a polynya edge characteristic originating at $t = t_0$ from a point $(X_0, V/UX_0)$ on L^- will advance with velocity **U** until it reaches the origin at a time $t = t_L$. For $t \geq t_L$ the characteristics will then follow the straight line path coinciding with the semi-infinite line $L^+ = \{(X, Y) : VX - UY = 0, X \geq 0\}$, which bounds the polynya to the west. Note that frazil ice trajectories will emanate from L^+. Similarly, a characteristic originating at $t = t_0$ from $(X_0, D + V/UX_0)$ on M^- will advance with velocity **U** until it reaches the point $(0, D)$ at a time $t = t_M$. For $t \geq t_M$ the characteristic will be affected by a nonzero flux of frazil ice coming from the island coastline. This characteristic will subsequently follow a progression similar to that of any other characteristic originating on the coastline.

To determine the evolution of characteristics originating on the coastline, we note that the frazil ice trajectory emanating from the origin (i.e., the semi-infinite line $l^+ = \{(x, y) : \mathfrak{V}x - uy = 0, x \geq 0\}$), divides the polynya domain into two regions, A to the east and B to the west (Fig. 5), in each of which the polynya solution can be easily derived. In region A, the advance of a polynya edge characteristic starting from ($X_0 = 0$, $0 < Y_0 < D$) at $t = t_0$ is given by (17) and (18), together with (13) and (14), with $h_{C0} = h_{B0} = 0$ (i.e., $p_0 = p_c = 1$). The characteristic will propagate westward until, at a time $t = t_l$, it intersects l^+ at the point (X_l, Y_l). At $t = t_l$, the characteristic enters region B in which the frazil ice flux emanates from the boundary L^+. In this region, a rotated reference frame, S_r, can be defined such that the negative y_r axis coincides with the line L^+, the transformation equations from S_r to S being

$$\begin{cases} X = \dfrac{-VX_r - UY_r}{|\mathbf{U}|}, & Y = \dfrac{UX_r - VY_r}{|\mathbf{U}|}; \\ u = \dfrac{-Vu_r - U\mathfrak{v}_r}{|\mathbf{U}|}, & \mathfrak{v} = \dfrac{Uu_r - V\mathfrak{v}_r}{|\mathbf{U}|}. \end{cases} \tag{23}$$

In S_r, the consolidated new ice velocity components are $U_r = 0$ and $V_r = -|\mathbf{U}|$. The evolution of a characteristic that has entered region B will again be given in the rotated system S_r by (13), (14), (17), and (18) after substitution of t_0, X_0, Y_0, and h_{C0} by t_l, X_{rl}, Y_{rl}, and h_{Cl}, respectively, where ($X_{rl} = u_rX_l/u$, $Y_{rl} = \mathfrak{V}_rY_l/\mathfrak{V}$) are the coordinates of the intersection point of the characteristic with l^+ in S_r, and $h_{Cl} = FX_{rl}/u_r$.

In summary, the evolution of the polynya edge characteristics is described by

$$\begin{cases} t - t_0 = \dfrac{1}{U}(X - X_0), & t \geq t_0, \quad (24a) \\ Y = \dfrac{V}{U}X, & t \geq t_0, \quad (24b) \end{cases}$$

in the case of a characteristic originating from L^-. When the characteristic originates from the coastline ($X_0 = 0$, $0 < Y_0 < D$), its evolution equations are

$$\begin{cases} t - t_0 = \dfrac{1}{u}X - (t_{ce} - t_{fe}) \ln\left(1 - \dfrac{X}{R_{oe}}\right), & t_0 \leq t < t_l, \quad (25a) \\ Y - Y_0 = \dfrac{v}{u}X + R_{ae} \ln\left(1 - \dfrac{X}{R_{oe}}\right), & t_0 \leq t < t_l, \quad (25b) \end{cases}$$

$$\begin{cases} t - t_l = \dfrac{1}{u_r}(X_r - X_{rl}) - t_{ce} \ln\left(\dfrac{X_r}{X_{rl}}\right), & t \geq t_l, \quad (25c) \\ Y_r = \dfrac{v_r}{u_r}X_r + t_{ce}|\mathbf{U}| \ln\left(\dfrac{X_r}{X_{rl}}\right), & t \geq t_l, \quad (25d) \end{cases}$$

where

$$\begin{cases} t_l - t_0 = \dfrac{1}{u}X_l - (t_{ce} - t_{fe}) \ln\left(1 - \dfrac{X_l}{R_{oe}}\right), \\ X_l = R_{oe}\left[1 - \exp\left(-\dfrac{Y_0}{R_{ae}}\right)\right]. \end{cases} \quad (26)$$

In (25) and (26), R_{oe} and R_{ae} are as given by (19) and (21), respectively, and $t_{ce} = R_{oe}/U$, $t_{fe} = R_{oe}/u$. Finally, when the characteristic starts from M^- it obeys

where

$$t_M - t_0 = -X_0/U \tag{28}$$

$$\begin{cases} t_l - t_M = \dfrac{1}{u}X_l - (t_{ce} - t_{fe}) \ln\left(1 - \dfrac{X_l}{R_{oe}}\right), \\ X_l = R_{oe}\left[1 - \exp\left(-\dfrac{D}{R_{ae}}\right)\right]. \end{cases} \tag{29}$$

The shape of the equilibrium polynya edge is given by (24b), (27d) (in region A), and (27f) (in region B). Figure 5 illustrates the polynya spinup to steady state in the presence of coastlines 20 and 40 km long. The consolidated and frazil ice speeds are $|\mathbf{U}| = 0.6$ m s^{-1} and $|\mathbf{u}| = 2|\mathbf{U}|$, respectively, the angle between the normal to the coastline and $\mathbf{U}$ is $\beta = +13°$, and $F = 0.27$ m day^{-1}. For both islands, the length scales R^e_o and R^e_a are ~ 19 and ~ 12 km, respectively. Note how the size of the island affects the polynya shape. When the coastline length is several times larger than R^e_a, the steady-state polynya width is close to the asymptotic value R^e_o. When the coastline length is comparable to or smaller than R^e_a, the polynya can open up to only a fraction of R^e_o.

Let us now determine the time taken for the polynya to reach equilibrium. We define the equilibrium timescale t_ϵ to be the time when the area of the polynya, A, reaches the value $A_e(1 - \epsilon)$, where $0 < \epsilon \ll 1$ and $A_e = [A]_{t=\infty} = DR_{oe}$. In the steady state, the areas occupied by the polynya in regions A and B are $A_{Ae} = A_e - R_{ae}R_{oe}[1 - \exp(-D/R_{ae})]$ and $A_{Be} = R_{ae}R_{oe}[1 - \exp(-D/R_{ae})]$, respectively. We wish to establish approximations for t_ϵ in the two limits: $A_{Ae}/A_e \approx 1$ (i.e., $D/R_{ae} \gg 1$) and $A_{Be}/A_e \approx 1$ (i.e., $D/R_{ae} \ll 1$). The timescale t_ϵ can in both cases be determined rigorously by considering the time evolution of A as described by (24) and (27). Nevertheless, we can estimate t_ϵ by using the following intuitive line of argument. If $A_{Ae}/A_e \approx 1$, then the polynya behavior will approximate that of a polynya in the presence of an infinite straight coast coinciding with the line $x = 0$. From (16), the timescale for equilibrium is then

$$t_\epsilon - t_0 \approx t_{fe} + \ln(\epsilon^{-1})(t_{ce} - t_{fe}), \qquad \frac{D}{R_{ae}} \gg 1. \tag{30}$$

If, on the other hand, $A_{Be}/A_e \approx 1$, the asymptotic polynya behavior will be similar to that of a polynya in the presence of an infinite straight coastline coinciding with the line L^+. In this limit, t_ϵ will again obey (16), but replacing t_{fe} ($=R_{oe}/u$) by 0 (since, along L^+, the asymptotic polynya width is 0), namely

$$t_\epsilon - t_0 \approx \ln(\epsilon^{-1})t_{ce}, \qquad \frac{D}{R_{ae}} \ll 1. \tag{31}$$

We have empirically observed that for an island of arbitrary length, $t_\epsilon - t_0$ is, in fact, well approximated by an area-weighted average of (30) and (31) (Fig. 6). The previous analysis demonstrates that the timescale for the opening of a wind-driven polynya adjacent to an island depends crucially on the relative magnitude of D and the alongshore adjustment length scale R_{ae}. Taking $\epsilon = 0.01$, and in the limit $U \longrightarrow u$, the time interval $t_\epsilon - t_0$ can be as much as 4.6 times longer for a small island ($D/R_{ae} \ll 1$) than for a large one ($D/R_{ae} \gg 1$).

2) RESPONSE OF A POLYNYA FROM AN ARBITRARY INITIAL STEADY STATE

We will now analyze the case when a steady-state polynya of nonzero initial area responds to an impulsive change in the atmospheric forcing. Rather than presenting in full detail the analytical solution of this problem, we will simply outline the way in which it can be obtained.

We consider an initial steady-state polynya for which the consolidated new ice velocity, frazil ice velocity, and frazil ice production rate are $\mathbf{U}_0$, $\mathbf{u}_0$, and F_0, respectively. At time $t = t_0$, these quantities change impulsively to $\mathbf{U}$, $\mathbf{u}$, and F, respectively. At this stage, it is useful to define a reference frame, S_s, which, at time $t = t_0$, coincides with the stationary frame S and which moves with velocity $\mathbf{U}$ with respect to S (i.e., the ice pack is stationary in S_s). Vector fields in S_s will be denoted by the subscript "s." With respect to frame S_s, the polynya edge velocity and the frazil ice velocity are parallel to

each other. Indeed, we see from (10) that the polynya edge evolves in S_s according to

$$\frac{dX_s}{dt} = -\frac{h_C}{H - h_C}u_s, \qquad \frac{dY_s}{dt} = -\frac{h_C}{H - h_C}v_s. \quad (32)$$

As a consequence, when **U** and **u** are spatially uniform and temporally constant, the equations governing the polynya edge become one-dimensional in S_s. A characteristic starting on a point **Q** of the polynya edge at $t = t_0$ will evolve along a straight line parallel to $\mathbf{u}_s = \mathbf{u} - \mathbf{U}$. The trajectories of frazil arriving at **Q** will also be parallel to $\mathbf{u}_s$. These trajectories may emanate from either the coastline, which recedes with velocity $-\mathbf{U}$ in S_s, or from a point, **P**, of frazil ice divergence on the polynya edge. From (32), **P** is stationary in S_s since at this point $h_C = 0$ for $t > t_0$. Note, however, that the initial frazil ice thickness at **P** is, in general, different from zero because **P** might have been a point of frazil ice convergence for $t < t_0$ (this is why we considered the general case $h_{B0} \geq 0$ in section 3a). If the initial distribution of frazil ice thickness is given, the polynya edge characteristics in S_s can be calculated following an approach similar to the one described in section 3a. The two major differences between this problem and the one discussed in section 3a are that 1) frazil ice can originate from moving boundaries (the land boundary) and 2) the initial distribution of frazil ice thickness will be, in general, piecewise linear rather than simply linear. However, these features can be introduced into the procedure presented in section 3a. The derivation of the polynya solution is then straightforward, albeit cumbersome. Instead, we will present numerical solutions of the problem.

In section 3a(3), we have shown that, in the presence of an infinite straight coastline, the behavior of the polynya strongly depends on the angle, Φ, between the consolidated new ice and frazil ice velocities. Clearly, this result also holds for the case of a polynya adjacent to an island. However, in this case the response of a steady-state polynya is additionally affected by the angle, Ψ, formed by the consolidated new ice velocity for $t < t_0$ and the relative velocity of frazil ice with respect to consolidated new ice for $t \geq t_0$. Specifically, if $\Psi > 0$, all points of the polynya edge that are points of ice convergence (divergence) for $t < t_0$ [i.e., the points on the eastern (western) boundary of the steady-state polynya] remain points of ice convergence (divergence) for $t > t_0$. In contrast, if $\Psi < 0$, there are regions of the polynya edge that are regions of ice convergence (divergence) for $t < t_0$, but which become regions of ice divergence (convergence) for $t \geq t_0$. In this latter case, the polynya generates leadlike structures that eventually detach from the main body of the polynya and follow an independent evolution. We will not discuss here the development of these structures. Nevertheless, one of them appears in the second case study presented in section 4b.

Figure 7 exemplifies the case when $\Psi > 0$. The experimental configuration is identical to that in Fig. 4e except that the coastline is a finite line segment 80 km long. For $t < t_0 = 0$ the polynya is in a steady state and the ice drift is characterized by the velocities $\mathbf{U}_0$ ($|\mathbf{U}_0| = 0.6$) and $\mathbf{u}_0$ ($|\mathbf{u}_0| = 2|\mathbf{U}_0|$). The frazil ice production rate is $F = 0.27$ m day^{-1}. In Fig. 7a, the dashed line represents the location of the polynya edge in quasi-equilibrium with the "old" forcing at $t < t_0$. In practice, this initial state was achieved by integrating the polynya equations over one day. At $t = t_0 = 0$ the wind changes direction and the ice velocities become $\mathbf{U}_1$ ($|\mathbf{U}_1| = |\mathbf{U}_0|$) and $\mathbf{u}_1$ ($|\mathbf{u}_1| = |\mathbf{u}_0|$). The polynya equations are then integrated for one more day. The angle between $\mathbf{U}_0$ and $\mathbf{u}_1 - \mathbf{U}_1$ is $\Psi \sim +10°$. The polynya adapts to the new forcing in two phases. The first phase lasts for ~1 h, during which the polynya edge retreats toward the coast (dash–dotted line). As explained in section 3a(3), this initial retreat results from the negative imbalance established initially between the consolidated new ice and frazil ice fluxes at the polynya edge. In the second phase, the flux imbalance changes sign and the polynya edge moves away from the coast (solid line) approaching its new equilibrium.

At time $t = 24$ h, the polynya has virtually reached a new steady state, as shown by the dashed line in Fig. 7b. The forcing then impulsively reverts to that applied for $t < t_0$ so that the ice drift regime is given by $\mathbf{U}_2$ (=$\mathbf{U}_0$) and $\mathbf{u}_2$ (=$\mathbf{u}_0$). The angle between $\mathbf{U}_1$ and $\mathbf{u}_2 - \mathbf{U}_2$ is $\Psi \sim +90°$. The polynya edge now gradually returns to its initial state at $t = t_0$, and, as in Fig. 7a, it does so in two phases: a rapid initial expansion that lasts for about 2 h (dashed–dotted line) followed by a comparatively slow contraction (solid line).

4. Application to the St. Lawrence Island polynya

The St. Lawrence Island polynya (SLIP) is a winter polynya that forms adjacent to the southern coast of St. Lawrence Island (Fig. 8). The SLIP is primarily driven by the prevailing northerly winds in the region (Pease 1987; Walter 1989; Kozo et al. 1990; Stringer and Groves 1991; Liu et al. 1997), although the weak shelf currents may also exert some control over the polynya (Lynch et al. 1997). Cavalieri and Martin (1994) distinguish two subregions in the SLIP, namely St. Lawrence east and St. Lawrence west, which are approximately separated by the 171°W meridian.

Brine rejection from the SLIP is a component of the regional salt budget and can affect the circulation in the vicinity of the polynya. Schumacher et al. (1983) have observed that, south of St. Lawrence Island, rapid U-turns of the current, from eastward to westward flow, can result from changes in the baroclinic structure of the water column during polynya opening events. It has also been suggested that, since the oceanographic circulation over the northern Bering Sea is dominated by a

northward flow, salty water created in the SLIP and other polynyas in the Bering Sea can contribute to the maintenance of the Arctic halocline (Aagaard et al. 1981).

Two assumptions made in our polynya model, namely that ice growth rates are almost exclusively determined by the surface energy budget, with no major contribution from oceanic heat sources, and that consolidated new ice motion is well described by a free-drift balance, are approximately satisfied in the SLIP. First, the depth of the shelf surrounding St. Lawrence Island is less than 30–40 m and, therefore, the winter water column will be well mixed. As a result, ice growth rates will be mainly controlled by surface cooling. Second, under the predominant northerly winds, internal stresses within the ice pack are likely to be small because the ice velocity field will be divergent. Consequently, the ice will move nearly in free drift. A third assumption made in the model, namely the spatial uniformity of the atmospheric forcing over the entire area of the polynya is less certain (see section 4b).

We will use the polynya theory described above to achieve the following two goals: First, to derive climatological estimates of monthly polynya extents and opening timescales. Second, to assess the model skill in portraying the short-term polynya response to atmospheric variability. To this effect, we will investigate three polynya opening events reported in the literature.

a. Determination of monthly polynya characteristics

To define realistic values for the long-term surface wind and frazil ice production over the SLIP, we have used the monthly mean climatology of surface air temperatures, dewpoints, and geostrophic winds of Crutcher and Meserve (1970) and the monthly mean climatology of cloudiness of Berliand and Strokina (1980). Using the parameterization (7) (see Fichefet and Morales Maqueda 1997), bulk surface heat fluxes were computed at the geographical location closest to the SLIP in the data. The parameterization of the shortwave radiation absorbed at the surface was that of Shine and Crane (1984). This parameterization discriminates between clear sky and overcast conditions. Climatological values for the cloud optical thickness were taken from Chou et al. (1981). The open water albedo formulations were those of Briegleb and Ramanathan (1982) and Kondratyev (1969) for clear sky and cloud-covered conditions, respectively. Finally, the atmospheric longwave radiation absorbed at the surface was formulated according to Marshunova (1966). This parameterization describes the effective atmospheric emissivity, e_a, as a linear function of cloudiness and a nonlinear function of surface water vapor pressure. Following Overland and Colony (1994), the surface wind, $\mathbf{U}_a$, was computed from the geostrophic wind, $\mathbf{U}_g$, by reducing $|\mathbf{U}_g|$ by factor of 0.8 and assuming that the angle between $\mathbf{U}_a$ and $\mathbf{U}_g$ is +32° (i.e., $\mathbf{U}_g$ is located to the right of $\mathbf{U}_a$). The climatological $\mathbf{U}_a$ turns out to be a persistent northeasterly wind throughout winter and spring, with month to month variations in wind direction of at most ±6°. The frazil ice and consolidated new ice velocities were obtained from the surface wind by using (8) and (9). In all simulations the frazil ice collection thickness was $H = 0.1$ m.

For each month during which the estimated frazil ice production rate, F, was positive, the polynya model was integrated to equilibrium, starting at time $t = t_0 = 0$, from a state in which no polynya existed. Table 1 shows the simulated equilibrium areal coverage of the SLIP, A_e, together with the observed median polynya areas, A_{obs}, and their 90% confidence intervals estimated by Stringer and Groves (1991). As indicated by these observational confidence intervals, the natural variability of the monthly polynya area can be quite large. Nevertheless, the equilibrium extent of the modeled SLIP agrees reasonably well with the values of the observed monthly areal range, except for May, when the observed polynya is much larger than the modeled one, and December, a month for which no data are provided. Cavalieri and Martin (1994) presented satellite-derived estimates of the annual-mean open water area south of St. Lawrence Island that hover above 5000 km^2, which is larger than the ~3550 km^2 average that can be obtained from Table 1. However, Cavalieri and Martin include all open water sources, such as open water holes in the consolidated new ice region (Pease 1987) and leads downwind of the polynya, in their calculations, which may explain the discrepancy.

Applying the flux balance principle, the equilibrium polynya area is given by

$$A_e = \frac{|\mathbf{U}|H}{F} D_{ef}, \qquad (33)$$

where D_{ef} is the "effective" cross-sectional length of the island (i.e., the maximum separation between coastline points in a direction perpendicular to the consolidated new ice motion; Fig. 9a). Clearly, for fixed $|\mathbf{U}|$, F, and H, the equilibrium area of the polynya will change, if the wind direction changes, because the effective cross section will be modified. In the case of St. Lawrence Island, D_{ef} can be as large as ~150 km, when $\mathbf{U}$ is directed to the south or south-southwest, and as small as ~60 km if $\mathbf{U}$ is directed to the east-southeast. However, because variations in the direction of the climatological winds are small, the range of values of D_{ef} in our simulations is less than 10 km, with D_{ef} being on average ~116 km.

From inspection of Table 1, it is apparent that A_e is better correlated with air temperatures than with wind velocity. Colder (warmer) weather produces smaller (larger) polynyas, whereas stronger (weaker) winds do not lead to a significant increase (decrease) in polynya size. This is in agreement with results presented by Pease (1987) and, as pointed out by this author, is due to the fact that decreasing (increasing) air temperatures increase (decrease) F, but not $|\mathbf{U}|$, while increasing (decreasing) wind speeds increase (decrease) both F and $|\mathbf{U}|$. Table 1 also shows the minimum and maximum values of

the equilibrium timescale, t_ϵ given by (30) and (31) ($\epsilon = 0.01$), respectively. These timescales correspond to the case of an idealized island whose coastline is a line segment of length D_{ef} oriented perpendicularly to **U**. The simulated equilibrium timescales fall within the interval (t^{min}_ϵ, t^{max}_ϵ). The simulated time for reaching equilibrium becomes closer to the lower (upper) bound of t_ϵ as the alongshore adjustment length scale, R_{ae} (also derived for the idealized island), decreases (increases) relative to D_{ef}, in agreement with the analysis presented in section 3b(1).

Figures 9a–d display the simulated SLIP in February, April, the first half of May, and December, respectively, at the moment when its extent attains a value of 99% of the equilibrium area. During the winter months, the SLIP almost splits into two individual sub-polynyas, which are approximately separated by the 171° meridian (line $Y = 0$ in the maps). As mentioned above, this is an observed feature of the SLIP. The existence of a SLIP-east and a SLIP-west in our model is the result of the polynya edge response to the island geometry. Because the offshore dimension of the polynya is of the order of 20 km or less, the polynya edge closely follows the coastline, and therefore, its width virtually shrinks to zero when the coastal boundary is aligned with **U**. However, we note that the simulated polynyas are markedly slanted to the west when compared with most observed ones. The reason for this is that, while the synoptic winds that drive polynya events are normally from the N or NNE [see Figs. 7 and 11 of Pease (1987) and Fig. 3 of Lynch et al. (1997)], the Crutcher and Meserve (1970) climatological winds tend to be northeasterly oriented. In April and May, a single polynya exists, which is considerably wider than the winter ones. As the distance between the polynya edge and the coast increases, so too does the alongshore adjustment length scale. Consequently, the polynya edge does not reproduce the fine structure of the coastline geometry. As pointed out by Kozo et al. (1990), the polynya edge adopts the shape of an airport windsock (Figs. 9b and 9c), tracking the predominant direction of the geostrophic wind. However, these spring polynyas expand so far to the south that the hypothesis of uniform wind and air temperature over the polynya area is invalid. The consolidated new ice will find higher air temperatures as it advances southward. This, combined with increased absorption of solar radiation, will lead to ice melting in the consolidated new ice region, even if frazil ice is still produced farther north. In addition, at this time of the year, the equilibrium timescale is significantly longer than a typical synoptic period of, say, 5 days. As a consequence, the real polynya will normally fail to reach equilibrium, which is in fact what has been observed (Kozo et al. 1990). This can explain the large discrepancy between our polynya area estimate for early May and that of Stringer and Groves (1991).

Figure 10 presents a plot of the polynya area versus time during a polynya opening event for each of the months under study. Since, for the duration of a polynya event, the frazil ice production, F, is assumed to be spatially uniform and constant in time, the net annual ice production, P (in m^3 of ice), is simply given by the integral of F times the area of the polynya over one year. Here, we are neglecting the fact that ice production will also be taking place in the consolidated new ice region. If we assume, as Schumacher et al. (1983) do, that the SLIP is open for about one-third of the time during periods when it can exist, and that a typical polynya event lasts for five days, then there will be a polynya opening twice per month from December to April and just one opening in May. Under these assumptions, the net volume of ice produced per month can be computed. The ice production amounts to 5–5.5 km^3 $month^{-1}$ from December to February and decays to 0.4 km^3 of ice in May, with a net annual ice production of ~ 22 km^3. This figure falls short from the estimate of 27–32 km^3 of ice per year cited by Cavalieri and Martin (1994). However, if heat fluxes over open water in the consolidated new ice region are assumed to be commensurate with those over the polynya and if the concentration of consolidated new ice oscillates between 70% and 50%, values of P comparable to those presented by Cavalieri and Martin (1994) can be retrieved.

b. Simulation of three SLIP opening events during February

Pease (1987) investigated two polynya openings that took place in February 1982 and February 1983. In 1982, the polynya started opening around 13 February, and observations over the polynya were carried out on 15 February. In 1983, the polynya opened from about 16 February, and measurements were made on 18 February. In both cases, atmospheric conditions were fairly constant during the opening process. Since the observations were in both cases performed about two days after the SLIP started to form, the polynya had probably reached equilibrium at that time.

In our simulation of these two polynya events, the net surface heat flux was derived as in Pease (1987). In particular, surface latent heat fluxes were neglected and upwelling longwave radiation was taken as 301 W m^{-2}. Table 2 lists the forcing parameters, together with the equilibrium timescales, alongshore length scales, and equilibrium polynya areas. In both years, measured wind speeds were larger and air temperatures colder than the climatological values. Therefore, frazil ice production rates were higher than those quoted in Table 1. In spite of this, the simulated polynya areas in these two cases turn out to be larger than the area of the February polynya derived from the climatological forcing. The increase in A_e found here is due to the larger effective cross-sectional length of the island, which results from the fact that the wind directions in the two case studies are significantly different from the climatological one. In February 1982, the wind was from the NNW and, in February 1983, it was from the NNE (Figs. 11a and 11b). In contrast, the climatological wind is from the NE, and since St. Lawrence Island offers a larger effective cross-sectional length to more northerly oriented winds, the value of D_{ef} is ~ 30–40 km larger in these experiments than in that of section 4a. The opening timescales (~ 1 day) and offshore widths (~ 10–20 km) of the simulated SLIP agree well with the estimates derived by Pease (1987) from NOAA Advanced Very High Resolution Radiometer images and aircraft observations, and the shape of the polynya edge and of the consolidated new ice–first-year ice regions shown in Fig. 11 are in qualitative agreement with contemporaneous satellite observations [see Fig. 3 of Walter (1989)]. In Fig. 11a, the relative velocity $\mathbf{u} - \mathbf{U}$ is such that, when the polynya begins to expand, some sections of the polynya edge turn out to be regions of frazil ice divergence. As explained in section 3b(2), temporary leads form in the presence of these features. The location of the coastal regions that induce lead formation at the polynya edge are indicated by the thick arrows. However, the leads have closed well before day 2 of the integration.

A second case study is provided by an opening event in February 1992, which has been investigated by Liu et al. (1997). By using wavelet analysis techniques, these authors tracked the evolution of the polynya and of the consolidated new ice region from 21 to 27 February. This event has also been studied by Lynch et al. (1997) with an atmosphere–sea ice coupled model. National Centers for Environmental Prediction and European Center for Medium-Range Weather Forecasts analysis for that period show that the geostrophic wind was from the NNE. In accordance with the assumption adopted in this study that both the pack ice and the consolidated new ice move at an angle of ~ 28° to the right of the surface wind (Overland and Colony 1994), we would have expected the ice drift to be approximately aligned with the geostrophic wind. This is not the case. In the leftmost panel of Fig. 12, we can see the trajectory of an ice floe that remained close to the consolidated new ice region during the entire period of observation. The trajectory is directed toward the south or south-southwest and the boundary between the first-year ice and the consolidated new ice regions is oriented in the north–south direction. We conclude therefore that, during this particular opening event, the ice drifted approximately in the direction of the surface wind. This behavior is at odds with the results of Kozo et al. (1990), who showed a good correlation between geostrophic wind direction and polynya orientation during mid–late March 1988. The origin of this discrepancy could be related to differences in the oceanic circulation during during the two periods. Lynch et al. (1997) showed that, despite the weakness of the oceanic circulation south of the St. Lawrence Island, the introduction of ocean currents in their simulations tended to increase the southward component of the ice drift during February 1992. A second possible reason for the discrepancy is that the ice internal stresses are more likely to play an important role in the ice drift in February, when the pack is compact, than in mid–late March, when the ice concentration has decreased and the ice will then tend to move in a regime closer to free drift.

In our simulation of this SLIP event we have assumed that both frazil ice and consolidated new ice motions are aligned with the surface wind, and we have deduced the wind direction from the motion of the ice floe displayed in Fig. 12. That **U** and **u** are parallel does not mean that the model becomes one-dimensional. Frazil ice and consolidated new ice drifts will still change direction in response to variations in the wind and, therefore, will not, in general, be described by rectilinear trajectories (Fig. 13c). The surface wind speed and air temperatures are the same as in Liu et al. (1997). Table 3 lists the forcing parameters and the simulated polynya characteristics at 2400 UTC 21, 24, and 27 February 1992. Surface heat fluxes were computed as in Pease (1987). The values of $t^{\min}_{e}$, $t^{\max}_{e}$, D_{ef}, R_{oe}, and A_e are the values that would be obtained if the polynya equations were integrated to equilibrium under a constant atmospheric forcing, equal to that stated for the corresponding day. Since the polynya is not in equilibrium, the actual polynya offshore length scale, R_o, and area, A, can be significantly different from R_{oe} and A_e. It is assumed that the polynya started opening at 0000 UTC 21 February. Increasing wind speeds lead to an increase in the ice export off the polynya over the first six days of integration. At the same time, the frazil ice production steadily decreases because of a warming of the weather. The polynya size, therefore, increases until it attains a maximum area of ~ 3900 km^2 at about 2400 UTC 26 February. On 27 February, air temperatures dropped by around 6° C and the polynya edge receded toward the coast.

Figures 13a–d show the modeled polynya for the same dates as in Fig. 12 and Table 3. The model successfully tracks the evolution of the boundary between the consolidated new ice and the first-year ice, but the active polynya region extends all along the coast of the island, whereas the observations suggest that this region was confined to the west of the 171° meridian (line $Y = 0$ in the maps). Liu et al. (1997) attribute the absence of Langmuir streak formation on the eastern part of the island to irregularities of the wind patterns on that side of the coast. Walter (1989) also found that, on 18 February 1983, frazil ice rows were located only west of 171.58°, with gray or gray/white young ice located to the east. This author shows that the topography of the island impacts on the atmospheric boundary layer over the SLIP, decreasing the wind speed and increasing the air temperature over the western part of the island. In order to model these effects, the hypothesis of uniform forcing fields should be abandoned. Finally, notice that Figs. 13c and 13d show that a narrow lead, ~ 15 km long and ~ 1 km in width, has formed on the eastern boundary of the polynya as a result of the wind veering on 27 February [see section 3b(2)]. The lead closes in ~ 9 h.

5. Summary and concluding remarks

We have presented a theory for the evolution of a two-dimensional wind-driven polynya. The theory is based on the ice flux balance principle of Lebedev (1968) and Pease (1987) in which the polynya evolution is governed by the balance between frazil ice and consolidated new ice fluxes at the polynya edge. To introduce time-dependence, the one-dimensional model of Ou (1988), which incorporates the effect of finite frazil ice drift, has been extended to two dimensions.

We have applied the model to the study of idealized polynyas in the presence of infinite- and finite-length straight coastlines under uniform time-varying atmospheric forcing. Four parameters have been found to play an important role in controlling the polynya behavior. The first two parameters are the consolidated new ice and the frazil ice timescales, t_{ce} and t_{fe}, respectively. The timescale t_{ce} determines the time that the polynya would take to grow frazil ice of thickness equal to the collection thickness. The timescale t_{fe} is the time required for frazil ice to cross the steady-state polynya width. The timescale for the polynya to reach the steady state increases (decreases) with increasing t_{ce} (t_{fe}). The other two parameters are the asymptotic polynya width, R_{oe}, and the alongshore adjustment length scale, R_{ae}: R_{oe} is the steady-state polynya width, and R_{ae} provides an estimate of the minimum length that a coastline feature, such as an embayment or a cape, must have in order that its shape is reproduced by the polynya edge. Polynya timescales and length scales are closely related. For example, the time taken for a polynya to open to a near-steady state on the lee side of an island will increase if R_{ae} is large compared with the effective cross-sectional length of the island.

The response of the modeled polynya to impulsive changes in wind direction presents two interesting and novel features.

First, when frazil ice and consolidated new ice are allowed to drift in different directions (as will, in general, be the case), short-period swings in the location of the polynya edge can take place. This is due to the fact that frazil ice and consolidated new ice drifts are assumed to respond instantaneously to changes in wind direction (in reality, the ice motion may lag the wind by one hour or so; see Ou 1988), whereas it takes a finite amount of time for the frazil ice thickness at the polynya edge to adapt to the new forcing. Thus, an instantaneous flux imbalance can be created at the polynya edge, which will result in an initial shoreward (seaward) motion of the polynya boundary, even when the equilibrium polynya width is larger (smaller) than the initial one. A second feature, is that narrow subpolynyas, or leads, can be generated if the change in wind direction is such that sections of the original polynya edge become regions of frazil ice divergence. The possible creation of leadlike structures of this kind in real polynyas deserves to be investigated.

The model has been applied to the investigation of seasonal and mesoscale variability in the St. Lawrence Island polynya. The model captures some of the observed characteristics of this polynya. For example, the presence of two almost independent polynyas during winter is reproduced by the model, and has been shown to result from changes in the orientation of the coastline relative to the prevailing southwestward ice transport. It is nevertheless likely that east–west contrasts in the wind and air temperature fields also play a role in the existence of the double-polynya system. It has also been demonstrated that the equilibrium area of the polynya depends not only on the wind speed and air temperature but also on the effective cross-sectional length of the island for a given direction of the consolidated new ice drift.

The model neglects a number of physical processes that are important in simulating the polynya behavior. We have assumed that the atmospheric forcing is spatially uniform. This is not the case for polynyas with large alongshore dimensions, such as the SLIP, because orographic features can modify the wind and air temperature fields over the polynya (Walter 1989). Also, for springtime polynyas, which extend far offshore, spatial variations in the surface heat budget will occur over the region, thereby creating nonuniform forcing. We have also neglected polynya–ocean interactions. We have assumed that the oceanic sensible heat flux into the polynya is negligible. This is obviously not acceptable if the polynya forms in a region of oceanic upwelling (Darby et al. 1994; Fichefet and Goosse 1999), or when a polynya extends beyond the continental shelf region. The effects of ocean currents on the ice drift have also been neglected. Ocean currents can introduce distortions in the simulated area and shape of the polynya (Lynch et al. 1997). In addition, baroclinic ocean currents can be enhanced by brine rejection during polynya opening events (Schumacher et al. 1983). Another simplification is that the frazil ice collection thickness is prescribed. This is an important shortcoming because, as a result, the effective ice export of the polynya is externally assigned, rather than determined by the model. To address this problem, parameterizations of H along the lines of those described by Martin and Kauffman (1981) and Bauer and Martin (1983) could be used.

Acknowledgments

We are grateful to L.-B. Tremblay and to anonymous reviewers for their comments on this work. We thank A. Looms for his assistance in the preparation of some of the diagrams. M. A. Morales Maqueda acknowledges support from a research grant awarded to A. J. Willmott and M. S. Darby via the 4th Round of the Antarctic Special Topic awards administered by the British Antarctic Survey (Natural Environment Research Council, United Kingdom).

REFERENCES

Aagaard, K., L. K. Coachman, and E. Carmack, 1981: On the halocline of the Arctic Ocean. *Deep-Sea Res.*, **28,** 529–545..

Bauer, J., and S. Martin, 1983: A model of grease ice growth in small leads. *J. Geophys. Res.*, **88,** 2917–2925..

Berliand, M. E., and T. G. Strokina, 1980: *Global Distribution of the Total Amount of Clouds* (in Russian). Hydrometeorological Publishing House, 71 pp..

Briegleb, B., and V. Ramanathan, 1982: Spectral and diurnal variations in clear sky planetary albedo. *J. Appl. Meteor.*, **21,** 1160–1171.. Find this article online

Cavalieri, D. J., and S. Martin, 1994: The contribution of Alaskan, Siberian, and Canadian coastal polynyas to the cold halocline layer of the Arctic Ocean. *J. Geophys. Res.*, **99,** 18 343–18 362..

Chou, S.-H., R. J. Curran, and G. Ohring, 1981: The effects of surface evaporation parameterizations on climate sensitivity to solar constant variations. *J. Atmos. Sci.*, **38,** 931–938.. Find this article online

Crutcher, H. L., and J. M. Meserve, 1970: Selected level heights, temperatures and dew points for the Northern Hemisphere. NAVAIR Rep. 50-1C-52, revised, U.S. Naval Weather Service Command, Washington, DC..

Darby, M. S., A. J. Willmott, and L. A. Mysak, 1994: A nonlinear steady state model of the North Water polynya, Baffin Bay. *J. Phys. Oceanogr.*, **24,** 1011–1020.. Find this article online

— ,— ,and T. Somerville, 1995: On the influence of coastline orientation on the steady state width of a latent heat polynya. *J. Geophys. Res.*, **100,** 13 625–13 633..

Fichefet, T., and M. A. Morales Maqueda, 1997: Sensitivity of a global sea ice model to the treatment of ice thermodynamics and dynamics. *J. Geophys. Res.*, **102,** 12 609–12 646..

— ,and H. Goosse, 1999: A numerical investigation of the spring Ross Sea polynya. *Geophys. Res. Lett.*, **26,** 1015–1018..

Haberman, R., 1998: *Elementary Applied Partial Differential Equations.* Prentice Hall, 736 pp..

Kondratyev, K. Y., 1969: *Radiation in the Atmosphere.* Academic Press, 912 pp..

Kozo, T. L., L. D. Farmer, and J. P. Welsh, 1990: Wind-generated polynyas off the coasts of the Bering Sea islands. *Sea Ice Properties and Processes. Proc. W. F. Weeks Sea Ice Symposium,* S. F. Ackley and W. F. Weaks, Eds., *CRREL Monogr.,* 126–132..

Lebedev, V. L., 1968: Maximum size of a wind-generated lead during sea freezing. *Oceanology,* **8,** 313–318..

Leibovich, S., 1983: The form and dynamics of Langmuir circulations. *Annu. Rev. Fluid Mech.,* **15,** 391–427..

Liu, A. K., S. Martin, and R. Kwok, 1997: Tracking of ice edges and ice floes by wavelet analysis of SAR images. *J. Atmos. Oceanic Technol.,* **14,** 1187–1198..

Lynch, A. H., M. F. Glueck, W. L. Chapman, D. A. Bailey, and J. E. Walsh, 1997: Satellite observation and climate system model simulation of the St. Lawrence Island polynya. *Tellus,* **49A,** 277–297..

Markus, T., and B. A. Burns, 1995: A method to estimate subpixel-scale coastal polynyas with satellite passive microwave data. *J. Geophys. Res.,* **100,** 4473–4487..

Marshunova, M. S., 1966: Principal characteristics of the radiation balance of the underlying surface and the atmosphere in the Arctic. *Soviet Data on the Arctic Heat Budget and its Climatic Influence,* J. O. Fletcher, B. Keller, and S. M. Olenicoff, Eds., The Rand Corporation, 51–131..

Martin, S., and P. Kauffman, 1981: A field and laboratory study of wave damping by grease ice. *J. Glaciol.,* **27,** 283–313..

Mysak, L. A., and F. Huang, 1992: A latent and sensible heat polynya model for the North Water, Northern Baffin Bay. *J. Phys. Oceanogr.,* **22,** 596–608.. Find this article online

Omstedt, A., and U. Svensson, 1984: Modeling supercooling and ice formation in a turbulent Ekman layer. *J. Geophys. Res.,* **89,** 735–744..

Ou, H. W., 1988: A time-dependent model of a coastal polynya. *J. Phys. Oceanogr.,* **18,** 584–590.. Find this article online

Overland, J. E., and R. L. Colony, 1994: Geostrophic drag coefficients for the central Arctic derived from Soviet drifting station data. *Tellus,* **46A,** 75–85..

Pease, C. H., 1987: The size of wind-driven coastal polynyas. *J. Geophys. Res.,* **92,** 7049–7059..

Schumacher, J. D., K. Aagaard, C. H. Pease, and R. B. Tripp, 1983:Effects of a shelf polynya on flow and water properties in the northern Bering Sea. *J. Geophys. Res.,* **88,** 2723–2732..

Shine, K. P., and R. G. Crane, 1984: The sensitivity of a one-dimensional thermodynamic sea-ice model to changes in cloudiness. *J. Geophys. Res.,* **89,** 10 615–10 622..

Smith, S. D., R. D. Muench, and C. H. Pease, 1990: Polynyas and leads: An overview of physical processes and environment. *J. Geophys. Res.,* **95,** 9461–9479..

Stringer, W. J., and J. E. Groves, 1991: Location and areal extent of polynyas in the Bering and Chuckchi Seas. *Arctic,* **44,** 164–171..

Wadhams, P., 1986: The seasonal ice zone. *The Geophysics of Sea Ice,* N. Untersteiner, Ed., NATO ASI Series, Series B, Physics, Vol. 146, Plenum Press, 825–991..

Walter, B. A., 1989: A study of the planetary boundary-layer over the polynya downwind of St-Lawrence-Island in the Bering Sea using aircraft data. *Bound.-Layer Meteor.,* **48,** 255–282..

Willmott, A. J., M. A. Morales Maqueda, and M. S. Darby, 1997: A model for the influence of wind and oceanic currents on the size of a steady-state latent heat coastal polynya. *J. Phys. Oceanogr.,* **27,** 2256–2275.. Find this article online

---

APPENDIX

6. Key to Most Relevant Variables and Subscripts

a. Variables:

A Area of the polynya [section 3b(1)]

D_{ef} Effective cross-sectional length of the island (section 4a)

F Frazil ice production rate

H Frazil ice collection thickness at the polynya edge

h Frazil ice thickness

h_B Frazil ice thickness at the origin of a frazil ice trajectory

h_C Frazil ice thickness at the polynya edge

$\mathbf{n}_C$ Horizontal unit vector perpendicular to the polynya edge

$p = 1 - h_C/H$ Normalized collection-minus-frazil ice thickness [section 3a(1)]

q_a Air specific humidity

$q_e = 1 - V/\mathfrak{V}$ Notation [section 3a(2)]

q_s Surface specific humidity

$\mathbf{R} \equiv (X, Y)$ Position vector of a point on the polynya edge

$\mathbf{r} \equiv (x, y)$ Position vector along a frazil ice trajectory

R_{ae} Alongshore adjustment length scale (21)

R_{oe} Offshore adjustment length scale (19)

T_a Air temperature

T_w Water temperature

t Time

t_c Critical time for response to an impulsive change in the forcing (14)

$t_{ce} = R_{oe}/U$ Consolidated new ice adjustment timescale [section 3a(1)]

$t_{fe} = R_{oe}/u$ Frazil ice adjustment timescale [section 3a(1)]

t_ϵ Equilibrium timescale (15)

$\mathbf{U} \equiv (U, V)$ Consolidated new ice velocity at the polynya edge

U_a Wind speed

$\mathbf{u} \equiv (u, \mathfrak{V})$ Frazil ice velocity

$\mathbf{u}_C \equiv (u_C, \mathfrak{V}_C)$ Frazil ice velocity at the polynya edge

Υ Consolidated new ice turning angle (section 2)

θ Frazil ice turning angle (section 2)

ϕ Angle between $\mathbf{U}$ and $\mathbf{u}_C$ [section 3a(3)]

ψ Angle between $\mathbf{U}$ for $t < t_0$ and $\mathbf{u} - \mathbf{U}$ for $t \geq t_0$ [section 3b(2)]

b. Subscripts:

0 Initial value at time $t = t_0$

c Value at time $t = t_c$

e Value at steady state

L Value on the line $L^{\pm}$ [section 3b(1)]

l Value on the line l^{+} [section 3b(1)]

M Value on the line $M^{\pm}$ [section 3b(1)]

r Value in the rotated reference frame S_r [section 3b(1)]

s Value in the reference frame S_s that moves with the ice pack [section 3b(1)]

ϵ Value at time $t = t_\epsilon$

Tables

Table 1. Simulated area of the SLIP using climatological forcing: U_a and ϕ_a are surface wind speed and direction (from N), respectively; T_a is surface air temperature; F is frazil ice production rate; T_ϵ is the polynya equilibrium timescale ($\epsilon = 0.01$); $t^{\min}_\epsilon$ and $t^{\max}_\epsilon$ are given in (30) and (31), respectively; t^{sim}_ϵ is the t_ϵ simulated by the model; D_{ef} is the effective cross-sectional length of the island (section 4*a*); R_{oe} and R_{ae} are the offshore and alongshore adjustment length scales (19 and 21), respectively; and A_e is the predicted equilibrium polynya area (33) and A_{obs} is the observed median value (after Stringer and Groves 1991).

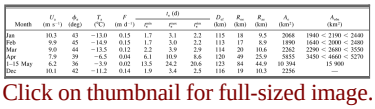

Click on thumbnail for full-sized image.

Table 2. Simulated area of the SLIP in February 1982/1983; U_a and ϕ_a are surface wind speed and direction (from N), respectively. T_a is surface air temperature. F is frazil ice production rate. t_ϵ is the polynya equilibrium timescale ($\epsilon = 0.01$); $t^{\min}_\epsilon$ and $t^{\max}_\epsilon$ are given in (30) and (31), respectively; t^{sim}_ϵ is the t_ϵ simulated by the model. D_{ef} is the effective cross-sectional length of the island (section 4*a*). R_{oe} and R_{ae} are the offshore and alongshore adjustment length scales (19 and 21), respectively. A_e is the predicted equilibrium polynya area (33).

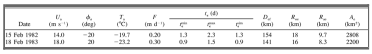

Click on thumbnail for full-sized image.

Table 3. Simulated area of the SLIP in February 1992: U_a and ϕ_a are surface wind speed and direction (from N), respectively. T_a is surface air temperature. F is frazil ice production rate. t_ϵ is the polynya equilibrium timescale ($\epsilon = 0.01$); $t^{\min}_\epsilon$ and $t^{\max}_\epsilon$ are given in (30) and (31), respectively. D_{ef} is the effective cross-sectional length of the island (section 4*a*). R_{oe} and R_o are the offshore adjustment length scale (19) and the simulated offshore length scale, respectively. A_e and A are the predicted equilibrium polynya area (33) and the simulated polynya area, respectively.

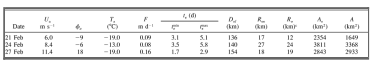

Click on thumbnail for full-sized image.

Figures

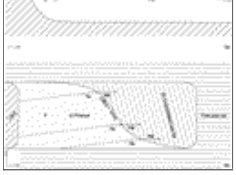

Click on thumbnail for full-sized image.

Fig. 1. Diagrams illustrating the polynya model in the one-dimensional (a) and two-dimensional cases (b). The frazil ice growth rate is F in the area of nearly open water adjacent to the coast, the polynya (i), and is transported with velocity **u** toward the polynya edge. The thickness of frazil ice is denoted by h. Frazil ice arriving at the polynya edge, $C(\mathbf{R}, t)$ = constant, piles up to a thickness H and moves into the consolidated new ice region (ii) with velocity **U**. In (b), the dotted lines represent frazil ice trajectories.

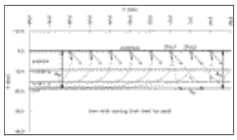

Click on thumbnail for full-sized image.

Fig. 2. Infinite straight coastline. At $t = t_0 = 0$ the polynya was closed. For $t_0 \leqslant t$ the ice drift regime becomes that depicted by the thick (**U**) and thin (**u**) vectors. The dashed lines are the polynya edge characteristics. At $t = t_\epsilon = 20.2$ h ($\epsilon = 0.01$), the polynya has virtually reached its steady state. The solid lines show the location of the polynya edge at $t = t_\epsilon/4$, $t = t_\epsilon/2$, and $t = \infty$. The length scales R_{oe} (~ 19 km) and R_{ae} (~ 12 km) are also shown.

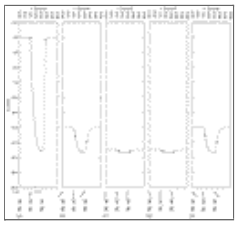

Click on thumbnail for full-sized image.

Fig. 3. Infinite straight coastline. Evolution of the polynya width (X) vs time (t) when $\phi = 0°$. In (a), for $t < t_0 = 0$ the ice drift is as represented by the thick ($\mathbf{U}_0$) and thin ($\mathbf{u}_0$) leftmost arrows (in arbitrary units). The angle between the normal to the coastline and $\mathbf{U}_0$ is $\beta = -90°$. At $t = t_0$, the ice drift regime changes to $\mathbf{U}_1$ and $\mathbf{u}_1$, with $\mathbf{U}_1$ perpendicular to the coast. When the polynya reaches equilibrium, the ice drift becomes $\mathbf{U}_2 = \mathbf{U}_0$ and $\mathbf{u}_2 = \mathbf{u}_0$. The long-dashed, solid, and short-dashed lines depict the evolution of X for each drift regime. The circles indicate the location of the polynya edge at $t = t_c$. Plots (b), (c), (d), and (e) are as (a), except $\beta = -39°$, $-13°$, $+13°$, and $+39°$, respectively.

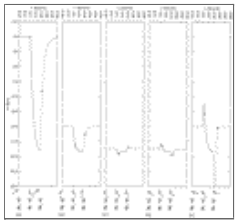

Click on thumbnail for full-sized image.

Fig. 4. As in Fig. 3 except $\phi = +28°$.

Click on thumbnail for full-sized image.

Fig. 5. Finite-length straight coastline. At $t = t_0 = 0$ the polynya was closed. For $t_0 \leqslant t$ the ice drift becomes that depicted by the thick (**U**) and thin (**u**) arrows. Solutions are shown for coastlines 20 (left) and 40 (right) km long. The dashed lines are the polynya edge characteristics given by (25) and (26). In both polynyas, $R_{oe} \sim 19$ km and $R_{ae} \sim 12$ km. For the left (right) polynya, t_ϵ ($\epsilon = 0.01$) is 30.2 h (25.4 h). The solid lines show the polynya edge at $t = t_\epsilon/4$, $t = t_\epsilon/2$, and $t = \infty$.

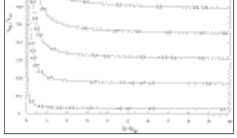

Click on thumbnail for full-sized image.

Fig. 6. Contours of $(t_\epsilon - t_0)/t_{ce}$ ($\epsilon = 0.01$) as a function of D/R_{ae} and t_{fe}/t_{ce} ($=U/u$) using the empirical formula $t_\epsilon - t_0 = A_{Ae}/A_e [t_{fe} + \ln(\epsilon^{-1})(t_{ce} - t_{fe})] + A_{Be}/A_e[\ln(\epsilon^{-1})t_{ce}]$.

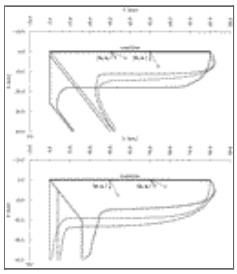

Click on thumbnail for full-sized image.

Fig. 7. Finite-length straight coastline. In (a), for $t < t_0 = 0$ the ice drift is as represented by the thick ($\mathbf{U}_0$) and thin ($\mathbf{u}_0$) arrows on the left. At $t = t_0 = 0$, the ice drift regime changes to that represented by the thick ($\mathbf{U}_1$) and thin ($\mathbf{u}_1$) arrows on the right. In (b), at $t = 24$ h the ice drift is impulsively reverted to the "old" regime ($\mathbf{U}_2 = \mathbf{U}_0$, $\mathbf{u}_2 = \mathbf{u}_0$). The dashed, dash–dotted, and solid lines in panel a (panel b) correspond to the location of the polynya edge at $t = 0$, 1, and 12 h ($t = 24$, 26, and 36 h), respectively.

Click on thumbnail for full-sized image.

Fig. 8. Geographical location of St. Lawrence Island.

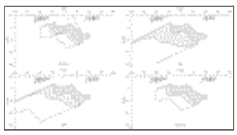

Click on thumbnail for full-sized image.

Fig. 9. Simulated SLIP (hatched area) at a time, t (counted from the moment the polynya started to open), when the polynya has reached 99% of its steady-state area in Feb (a), Apr (b), May (c), and Dec (d). Also shown is the consolidated new ice region (nonhatched area). Within the polynya, the dashed lines are frazil ice trajectories drawn about 10 km apart. The thick (thin) vector represents the consolidated new ice (frazil ice) velocity. The small blank areas adjacent to the coast correspond to landfast ice.

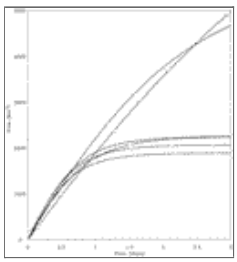

Click on thumbnail for full-sized image.

Fig. 10. Area of the SLIP vs time during an opening event under climatological forcing typical of Jan (J), Feb (F), Mar (Mr), Apr (A), May (My), and Dec (D).

Click on thumbnail for full-sized image.

Fig. 11. As in Fig. 10 except for short timescale atmospheric conditions on 13–15 Feb 1982 (a) and on 16–18 Feb 1983 (b). The state of the polynya is shown two days after it started to open. (a) The thick arrows indicate the location of coastal regions that induce lead formation at the polynya edge.

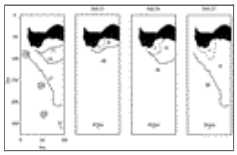

Click on thumbnail for full-sized image.

Fig. 12. Diagram of the observed evolution of the SLIP from 21 to 27 Feb 1992. The solid lines depict the boundary between the first-year ice and the consolidated new ice regions. The closed contours on the leftmost panel correspond to the successive positions of a particular ice floe. In the three panels on the right, the active polynya region is area I, the consolidated new ice regions is area II, and the first-year pack is area III. Redrawn from Liu et al. (1997).

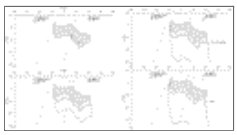

Click on thumbnail for full-sized image.

Fig. 13. As in Fig. 10, except for short timescale atmospheric conditions on 21–27 Feb 1992. The polynya started opening at 0000 UTC on 21 Feb ($t = t_0 = 0$ d, 0 h). The area within the rectangle approximately coincides with the Synthetic Aperture Radar (SAR) imagery domain shown in Fig. 13. Changes in wind direction and speed occurred at $t = 3$ d, 0 h and at $t = 6$ d, 0 h. Frazil ice trajectories in (c) are not straight lines because the frazil ice arriving at the polynya edge has crossed the polynya under two different wind regimes, namely before and after $t = 6$ d, 0 h.

* Current affiliation: Potsdam Institute for Climate Impact Research, Potsdam, Germany.

Corresponding author address: Dr. M. A. Morales Maqueda, Potsdam Institute for Climate Impact Research, P.O. Box 60 12 03, 14412 Potsdam, Germany.

E-mail: maqueda@pik-potsdam.de

top